





Targeted Inhibition of Purine Metabolism Is Effective in Suppressing Hepatocellular Carcinoma Progression

Yong Chun Chong ¹, Tan Boon Toh ^{2,3}, Zhiling Chan,¹ Quy Xiao Xuan Lin ³, Dexter Kai Hao Thng,³ Lissa Hooi,³ Zhaobing Ding,¹ Timothy Shuen,⁴ Han Chong Toh,⁴ Yock Young Dan,⁵ Glenn Kunnath Bonney,⁶ Lei Zhou,⁷ Pierce Chow,⁸ Yulan Wang,⁹ Touati Benoukrif ^{3,10}, Edward Kai-Hua Chow,³ and Weiping Han¹

Tumor-specific metabolic rewiring, acquired to confer a proliferative and survival advantage over nontransformed cells, represents a renewed focus in cancer therapy development. Hepatocellular carcinoma (HCC), a malignancy that has hitherto been resistant to compounds targeting oncogenic signaling pathways, represents a candidate cancer to investigate the efficacy of selectively antagonizing such adaptive metabolic reprogramming. To this end, we sought to characterize metabolic changes in HCC necessary for tumorigenesis. We analyzed gene expression profiles in three independent large-scale patient cohorts who had HCC. We identified a commonly deregulated purine metabolic signature in tumors with the extent of purine biosynthetic enzyme up-regulation correlated with tumor grade and a predictor of clinical outcome. The functional significance of enhanced purine metabolism as a hallmark in human HCC was then validated using a combination of HCC cell lines, patient-derived xenograft (PDX) organoids, and mouse models. Targeted ablation of purine biosynthesis by knockdown of the rate-limiting enzyme inosine-5'-monophosphate dehydrogenase (*IMPDH*) or using the drug mycophenolate mofetil (MMF) reduced HCC proliferation *in vitro* and decreased the tumor burden *in vivo*. In comparing the sensitivities of PDX tumor organoids to MMF therapy, we found that HCC tumors defined by high levels of *IMPDH* and guanosine nucleosides were most susceptible to treatment. Mechanistically, a phosphoinositide 3-kinase (PI3K)–E2F transcription factor 1 (E2F1) axis coordinated purine biosynthetic enzyme expression, deregulation of which altered the activity of mitogen-activated protein kinase/RAS signaling. Simultaneously abolishing PI3K signaling and *IMPDH* activity with clinically approved inhibitors resulted in greatest efficacy in reducing tumor growth in a PDX mouse model. **Conclusion:** Enhanced purine metabolic activity regulated by PI3K pathway-dependent activation of E2F1 promotes HCC carcinogenesis, suggesting the potential for targeting purine metabolic reprogramming as a precision therapeutic strategy for patients with HCC. (*Hepatology Communications* 2020;4:1362-1381).

Hepatocellular carcinoma (HCC) is the most prevalent form of primary liver cancer and accounts for the second highest number of cancer mortalities worldwide.⁽¹⁾ Despite the global burden, surgical resection and liver transplantation remain the only curative treatments,⁽²⁾ and existing therapies for advanced unresected HCC offer modest survival benefits.^(3,4) Several inhibitors that

Abbreviations: ADSL, adenylosuccinate lyase; ADSS, adenylosuccinate synthetase; AICAR, 5-aminoimidazole-4-carboxamide-1- β -D-ribofuranoside; AKT, protein kinase B; AMP, adenosine monophosphate; ATIC, 5-aminoimidazole-4-carboxamide ribonucleotide formyltransferase; c, cyclic; CREB, cyclic adenosine monophosphate responsive element binding protein; Ctrl, control; DEN, diethylnitrosamine; DMSO, dimethyl sulfoxide; E2F1, E2F transcription factor 1; GART, phosphoribosylglycinamide formyltransferase, phosphoribosylglycinamide synthetase, phosphoribosylaminoimidazole synthetase; GMP, guanosine monophosphate; GMPS, guanine monophosphate synthase; HCC, hepatocellular carcinoma; HSP90, heat shock protein 90; IC50, median inhibitory concentration; IMP, inosine monophosphate; IMPDH, inosine-5'-monophosphate dehydrogenase; LIHC, liver hepatocellular carcinoma; MAPK, mitogen-activated protein kinase; MMF, mycophenolate mofetil; MPA, mycophenolic acid; mRNA, messenger RNA; mTOR, mammalian target of rapamycin; MYC, myelocytomatosis; NSG, NOD scid gamma; PAICS, phosphoribosylaminoimidazole carboxylase and phosphoribosylaminoimidazolesuccinocarboxamide synthase; PDX, patient-derived xenograft; PEAS, phosphoribosylformylglycinamide synthase; PI3K, phosphoinositide 3-kinase; PPAT, phosphoribosyl pyrophosphate amidotransferase; PRPS1, phosphoribosyl pyrophosphate synthetase 1; qPCR, quantitative polymerase chain reaction; RB, RB transcriptional corepressor; SGH, Singapore General Hospital; sh, short hairpin; TCGA, The Cancer Genome Atlas; TF, transcription factor; XMP, xanthosine monophosphate.

Received April 22, 2020; accepted June 10, 2020.

Additional Supporting Information may be found at onlinelibrary.wiley.com/doi/10.1002/hep4.1559/supinfo.

have demonstrated clinical benefits in other cancers, such as sunitinib and erlotinib, as well as yttrium-90 radioembolization fail to show positive effects in patients,⁽⁵⁾ highlighting the dearth of available treatments and a need to identify new modalities for clinical intervention in HCC. Cancer metabolism offers an attractive target to selectively antagonize tumors given that tumor cells exhibit altered metabolism to gain a survival advantage over nontransformed cells.⁽⁶⁾ Metabolic reprogramming of tumors to consume glucose and divert these metabolic intermediates into lactate production, a phenomenon known as aerobic glycolysis or the Warburg effect, was one of the first reported distinctions between cancer and normal tissues.⁽⁷⁾ Rewiring of amino acid, lipid, and nucleotide metabolism has also been shown to be essential for sustaining tumorigenesis in various cancers,⁽⁶⁾ suggesting a benefit of exploiting metabolic liabilities for cancer therapy. Deregulation of tumor metabolism is often achieved by alterations in the expression of metabolic enzymes either by gene amplification or deletion or as a consequence of changes in the activation status of upstream growth signaling pathways.⁽⁸⁾ The purine biosynthesis pathway has been demonstrated

to be under the transcriptional control of myelocytomatosis (MYC) signaling in cancers, such as glioma, melanoma, lymphoma, and prostate cancer.⁽⁹⁻¹²⁾ Insofar as purine metabolism has been implicated in maintaining tumor-initiating cells and the pathogenesis of various malignancies through enhancing nucleic acid synthesis to sustain rapid proliferation,^(9,13) a role for purine biosynthesis in HCC has remained inconclusive.

Inosine-5'-monophosphate dehydrogenase (IMPDH) is a critical enzyme that catalyzes the conversion of inosine monophosphate (IMP) to xanthosine monophosphate (XMP), an irreversible and rate-limiting process during purine biosynthesis that establishes the intracellular pool of guanine nucleotides.⁽¹⁴⁾ IMPDH activity is enhanced in tumor cells, with IMPDH a potential chemotherapy target.^(15,16) Two IMPDH inhibitors, mycophenolic mofetil (CellCept) and mycophenolate sodium (Myfortic), are used as immunosuppressants in organ transplants and autoimmune diseases.^(17,18) Clinical trials to assess the efficacy of CellCept in cancers have been confined to hematologic malignancies, and investigations into the therapeutic benefit of inhibiting purine biosynthesis in solid cancers are lacking.

*Supported by the A*STAR Biomedical Research Council (intramural funding to W.H.), the Cancer Science Institute of Singapore (intramural funding to E.K.-H.C.), and the National Medical Research Council, Singapore (Young Individual Research Grant #OFYIRG17may044 to Y.C.C.).*

© 2020 The Authors. Hepatology Communications published by Wiley Periodicals LLC on behalf of American Association for the Study of Liver Diseases. This is an open access article under the terms of the Creative Commons Attribution-NonCommercial-NoDerivs License, which permits use and distribution in any medium, provided the original work is properly cited, the use is non-commercial and no modifications or adaptations are made.

View this article online at wileyonlinelibrary.com.

DOI 10.1002/hep4.1559

Potential conflict of interest: Nothing to report.

ARTICLE INFORMATION:

From the ¹Singapore Bioimaging Consortium, Agency for Science, Technology, and Research, Singapore, Singapore; ²The N.1 Institute for Health; ³Cancer Science Institute of Singapore, National University of Singapore, Singapore, Singapore; ⁴Division of Medical Oncology, National Cancer Center Singapore, Singapore, Singapore; ⁵Division of Gastroenterology and Hepatology; ⁶Division of Hepatobiliary and Liver Transplantation Surgery, National University Health System, Singapore, Singapore; ⁷Department of Medicine, National University of Singapore, Singapore, Singapore; ⁸Department of Hepatopancreatobiliary and Transplant Surgery, Singapore General Hospital, Singapore, Singapore; ⁹Singapore Phenome Center, Lee Kong Chian School of Medicine, Nanyang Technological University, Singapore, Singapore; ¹⁰Discipline of Genetics, Faculty of Medicine, Memorial University of Newfoundland, St. John's, Canada.

ADDRESS CORRESPONDENCE AND REPRINT REQUESTS TO:

Weiping Han, Ph.D.
Laboratory of Metabolic Medicine
Singapore Bioimaging Consortium
#02-02 Helios, 11 Biopolis Way

Singapore 138667, Singapore
E-mail: wh10@cornell.edu
Tel.: +65 6478 8721

Large-scale HCC cohort studies, such as The Cancer Genome Atlas (TCGA), highlight extensive interpatient tumor heterogeneity in terms of gene expression levels and oncogenic mutations, indicating a patient-specific tumor profile and illustrating the complexities of a one-size-fits-all approach.⁽¹⁹⁾ Although common mutations in telomerase reverse transcriptase (*TERT*), tumor protein p53 (*TP53*), and catenin beta 1 (*CTNNB1*) exist in most patients, these molecular alterations are not clinically druggable. The promise of precision medicine in oncology has resulted in tailor-made treatments based on tumor molecular profile instead of tumor origin.⁽²⁰⁾ Despite advances across tumor types, the development of molecularly targeted therapeutics is missing in HCC due to the absence of validated biomarkers to predict treatment outcome.⁽²¹⁾ Here, we provide evidence that inhibition of purine biosynthesis by targeting IMPDH in HCCs distinguished by high purine biosynthetic activity reduced the tumor burden. In combination with an antagonist of phosphoinositide 3-kinase (PI3K), an upstream regulator of purine biosynthetic enzyme expression, to potently suppress purine metabolism, we observed an enhanced reduction in tumorigenesis, offering a novel combination for precision therapy of HCC.

Materials and Methods

HUMAN SUBJECTS AND DATA

Protocols involving human patients were approved by the SingHealth Institutional Review Board at the National Cancer Center Singapore (NCCS). Tumor samples were surgically removed at the NCCS with informed consent from the patients. TCGA-liver hepatocellular carcinoma (LIHC) gene expression data and clinical parameters were downloaded from the University of California Santa Cruz Cancer Genomics Browser (<https://xenabrowser.net/>) and cBioPortal for Cancer Genomics (<https://www.cbioportal.org/>). Data from the Roessler Liver 2 data set were downloaded from the OncoPrint platform (<https://www.oncoprint.org/resource/login.html>) with default thresholds set for *P* values and gene ranks. Gene expression data of HCC cell lines were downloaded from the Cancer Cell Line Encyclopedia (CCLE) portal (<https://portals.broadinstitute.org/ccle>).

ANIMALS AND TUMOR XENOGRAFT MODEL

All animal studies were approved by the institutional animal care and use committees at A*STAR and the National University of Singapore. We purchased 6-8-week-old male C57BL/6, female CrTac:NCr-Foxn1^{athymic nude (nu)}, and female NOD.Cg-Prkdc^{severe combined immunodeficiency (scid)}112rg^{tm1Wjl/SzJ} (NOD *scid* gamma [NSG]) mice from InVivos, Singapore. All mice were maintained under pathogen-free conditions on a 12-hour light/dark cycle with free access to water and standard chow diet (1324; Altromin). To chemically induce HCC, 5 mg/mL diethylnitrosamine (DEN) (N0258; Sigma) was injected intraperitoneally into 2-week-old C57BL/6 mice at a dose of 20 mg/kg body weight, followed by eight consecutive administrations of 1,4-Bis[2-(3,5-dichloropyridyloxy)]benzene (TCPOBOP) (T1443; Sigma) at a dose of 3 mg/kg body weight every 14 days starting at 4 weeks of age. At 7 months, tumor size and multiplicity were evaluated by counting the number of visible tumor nodules and determining the largest diameter of each nodule with a caliper. For the tumor xenograft model, 10⁶ cells in 100 μ L Dulbecco's modified Eagle's medium (DMEM) were mixed with an equal volume of Matrigel (354230; Corning) and injected subcutaneously into the hind flank of 6-8-week-old nude/NSG mice. Tumor growth was allowed to proceed for a month. Mice with no tumors were not used for analysis. The tumor burden was determined by measuring tumor weight and volume (*V*), where $V = (\text{tumor length} \times \text{tumor width} [W] \times W)/2$. For patient-derived xenograft (PDX) experiments, freshly resected human HCC tissues were transplanted subcutaneously into NSG mice. Mice were euthanized when tumors reached 1.5 cm in dimension. PDX tumors were subsequently harvested and processed into PDX cells, as described.⁽²²⁾ PDX tumors were maintained as a continuous source of tumor cells using NSG mice. For drug treatment of tumors, mycophenolate mofetil (MMF) was resuspended in a vehicle comprising 0.9% sodium chloride, 0.5% methyl cellulose, and 0.4% TWEEN 80, while the PI3K inhibitor PI-103 was dissolved in dimethyl sulfoxide (DMSO). One week after tumor cell injection, mice were administered a regimen of 120 mg/kg MMF by oral gavage twice a day and 10 mg/kg PI-103 by intraperitoneal injection daily for 3 weeks.

Results

DE NOVO PURINE BIOSYNTHESIS IS UP-REGULATED IN HCC

Previous studies demonstrated that dysregulation of hepatic metabolism is crucial for the development and progression of liver disease.^(23,24) To identify metabolic pathways essential for HCC tumorigenesis, we assessed the gene expression pattern of key enzymes involved in cellular metabolism in patients from the TCGA-LIHC data set. We found that enzymes in the *de novo* purine biosynthesis pathway showed a significant increase across 360 HCC tumor samples compared to nontransformed liver (Fig. 1A). In contrast, we did not observe a consistent differential up-regulation of enzymes in four other core metabolic pathways: glycolysis, glutathione, one carbon metabolism, and pyrimidine (Supporting Fig. S1A). Increased expression of enzymes in the pentose phosphate pathway (PPP) in tumors, however, suggested enhanced levels of ribose 5-phosphate (R5P), a core product and intermediate of the PPP that is also a critical precursor for purine biosynthesis. Purine metabolism is initiated by the sequential activities of several enzymes, such as phosphoribosyl pyrophosphate amidotransferase (PPAT), phosphoribosylformylglycinamide synthase (PFAS), and 5-aminoimidazole-4-carboxamide ribonucleotide formyltransferase (ATIC)/IMP cyclohydrolase, functioning in the main branch leading to stepwise formation of IMP from R5P. IMP can then be converted into adenosine monophosphate (AMP) or guanosine monophosphate (GMP) through two distinct reactions catalyzed by adenylosuccinate lyase (ADSL), and IMPDH and guanine monophosphate synthase (GMPS), respectively (Supporting Fig. S1B). Higher grade tumors (G2 and G3), pathologically defined as poorly differentiated and highly metastatic, exhibit progressively higher levels of *PFAS*, *ATIC*, *IMPDH1*, *IMPDH2*, *GMPS*, and *ADSL* compared to low-grade tumors (G1) or normal liver tissue (Supporting Fig. S1C). We also determined that stage T2 and T3 tumors, clinically manifested as large tumors with high multiplicity, were characterized by up-regulated expression of these enzymes (Supporting Fig. S1D). Consistent with a critical role for enhanced purine biosynthesis in the pathogenesis of aggressive HCC, high expression of these enzymes correlated with poor patient survival outcome (Fig. 1B). Further

interrogation of transcriptomic data from tumor and matched normal tissue of a cohort of 48 patients with HCC from the Singapore General Hospital (SGH) revealed a corresponding enrichment of purine biosynthetic enzymes in tumors (Fig. 1C). Analysis of the Roessler human HCC data set comprising 220 normal and 225 tumor samples on the OncoPrint platform^(25,26) also confirmed that expression of purine biosynthetic genes was significantly up-regulated in tumors (Fig. 1D). Surprisingly, we did not find any correlation between overall patient survival and tumor levels of *IMPDH1* or *IMPDH2* (Supporting Fig. S2) in 11 other gastrointestinal cancers in the TCGA, suggesting a specific dependence on purine biosynthesis for HCC growth and sustenance.

IMPDH ACTIVITY IS NECESSARY FOR HCC PROLIFERATION

Elevated expression of purine biosynthetic enzymes in HCC suggests that HCC may be sensitive to inhibition of purine metabolism. To this end, we targeted the first committed and rate-limiting step in guanine nucleotide biosynthesis by using MMF, a U.S. Food and Drug Administration-approved prodrug of mycophenolic acid (MPA) that inhibits IMPDH activity, in a chemically induced mouse model of HCC. DEN-induced tumors expressed elevated levels of both IMPDH isoforms compared to adjacent nontransformed liver (Supporting Fig. S3A). Tumors were visibly smaller after a 3-week regimen of MMF (Fig. 2A). Despite a decrease in tumor size (Fig. 2B), we did not observe an effect of MMF on the frequency of tumor formation (Fig. 2C). We next turned to an HCC cell line model to elucidate the mechanisms regulating purine biosynthesis. To select an optimal HCC line that demonstrates maximal response to MPA, we mined the CCLE database to identify cell lines with highest expression levels of purine biosynthetic enzymes.⁽²⁷⁾ Clustering analysis resulted in the segregation of 25 HCC cell lines into two distinct groups with contrasting expression profiles (Supporting Fig. S3B). Because MPA directly targets both IMPDH isoforms, we validated by quantitative polymerase chain reaction (qPCR) that Huh7 cells expressed highest levels of both *IMPDH1* and *IMPDH2* (Supporting Fig. S3C,D). Treatment of Huh7 cells with MPA completely attenuated the proliferation of these cells

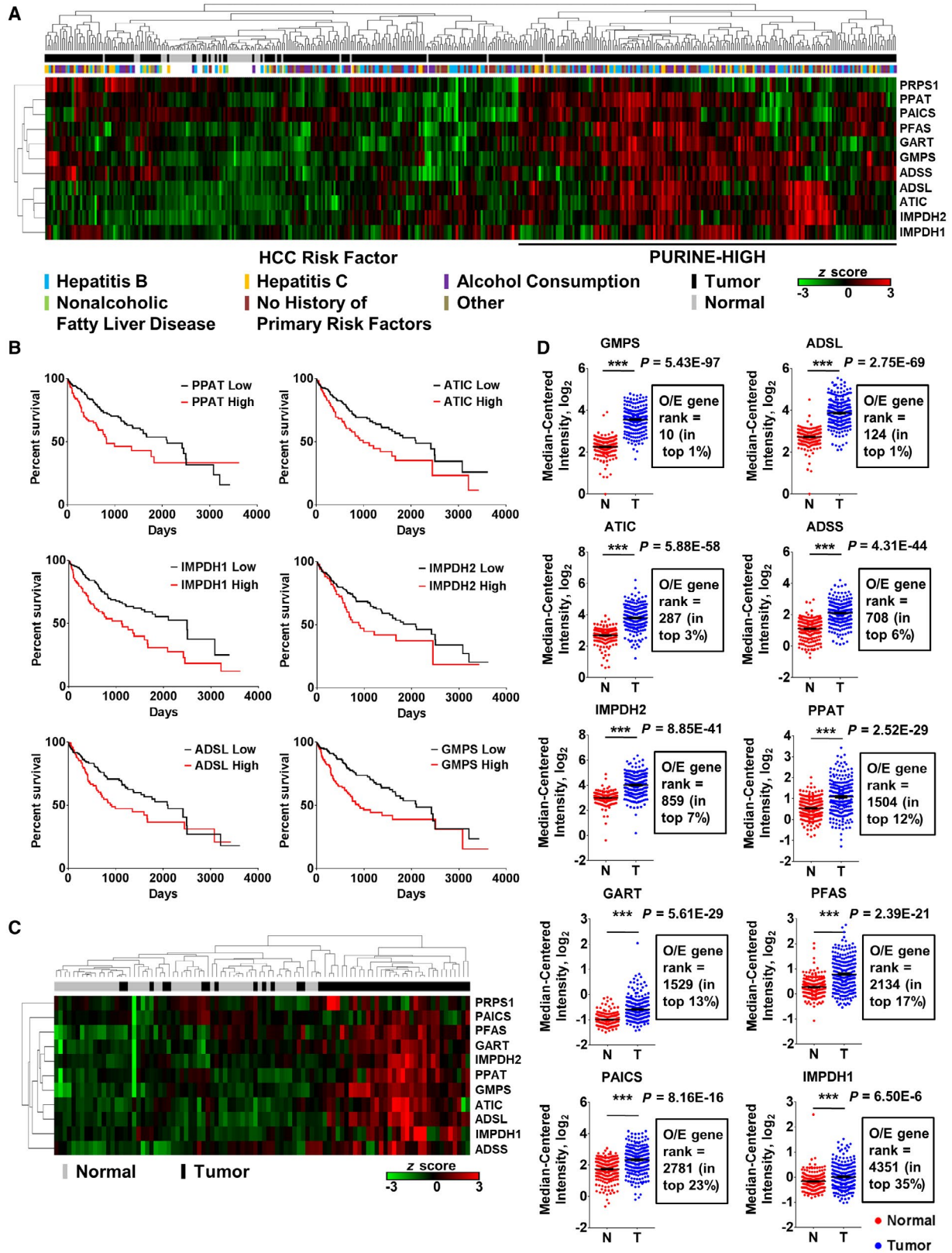


FIG. 1. Purine biosynthesis pathway gene expression is up-regulated in HCC. (A) Heatmap showing relative transcript levels of *de novo* purine biosynthesis pathway genes in TCGA-LIHC samples. Z scores were calculated from the \log_2 transformed FPKM values for each sample. Purine-high samples denote a cluster of HCC with universally elevated enzyme expression. (B) Kaplan-Meier survival curves of overall patient survival according to expression levels of purine biosynthesis pathway genes. Log-rank test. (*PPAT*^{low}, n = 233; *PPAT*^{high}, n = 123; *P* = 0.0012. *ATIC*^{low}, n = 236; *ATIC*^{high}, n = 120; *P* = 0.0022. *IMPDH1*^{low}, n = 235; *IMPDH1*^{high}, n = 121; *P* = 0.0001. *IMPDH2*^{low}, n = 264; *IMPDH2*^{high}, n = 92; *P* = 0.021. *ADSL*^{low}, n = 239; *ADSL*^{high}, n = 117; *P* = 0.0095. *GMP5*^{low}, n = 214; *GMP5*^{high}, n = 142; *P* < 0.0001). (C) Heatmap showing relative transcript levels of *de novo* purine biosynthesis pathway genes in tumor and matched normal samples from a cohort of 48 SGH patients. (D) Expression levels of purine biosynthesis pathway genes from the Roessler et al. data set in the Oncomine database. The extent of up-regulation of each enzyme in tumors relative to normal tissues is indicated by its overexpression gene rank. Nontumor, n = 220; tumor, n = 225; data are mean \pm SEM; ****P* < 0.001. Abbreviations: FPKM, fragments per kilobase of transcript per million mapped reads; N, nontumor; O/E, overexpression; T, tumor.

(Fig. 2D), a phenomenon reversed by exogenous addition of guanine or guanosine (Fig. 2E), consistent with studies demonstrating that the only nucleotides that had intracellular levels reduced by MPA treatment were guanylates.⁽²⁸⁾

We generated stable knockdowns of both IMPDH isoforms in Huh7 cells by using three independent short hairpin (sh)RNA sequences (Supporting Fig. S3E-G). Reduction of either *IMPDH1* or *IMPDH2* decreased cellular proliferative capacity (Fig. 2F), a phenomenon reversed by exogenous supplementation of guanine or guanosine (Supporting Fig. S3H). Treatment of *IMPDH* knockdown cells by MPA further attenuated their proliferation (Supporting Fig. S3I). These cells also displayed impaired tumorigenic activity when xenografted into nude mice (Fig. 2G,H). Similarly, *IMPDH1* or *IMPDH2* knockdown in SNU398 cells impacted their proliferation (Supporting Fig. S3J-M). Treatment of SNU398 cells with MPA also abolished their proliferative capacity, a phenomenon that was reversed by guanine or guanosine (Supporting Fig. S3N). In support of purine synthetic activity being critical for the growth and proliferation of HCC cells with elevated expression of IMPDH, HepG2 cells, which express comparatively low levels of both *IMPDH1* and *IMPDH2*, were resistant to MPA (Supporting Fig. S3O). In addition to its catalytic role in the conversion of IMP to XMP, IMPDH is also capable of binding nucleic acids and regulating transcription, a function exclusively mediated by its Bateman domain, a moiety dispensable for the enzymatic activity of IMPDH.^(29,30) To explore a contribution by this noncatalytic feature toward the tumorigenic potential of IMPDH, we constructed *IMPDH1* mutants lacking the Bateman domain (Supporting Fig. S4A) and overexpressed them in *IMPDH1*-knockdown Huh7 cells (Supporting Fig. S4B). Restoration of cellular proliferation was

observed in cells transduced with Bateman-deficient *IMPDH1* (Fig. 2I). The lack of a functional role for the Bateman domain in tumorigenesis was confirmed using two *IMPDH1* isoforms: canonical *IMPDH1* expressed ubiquitously (isoform E) and a longer isoform containing an additional exon at the amino terminus (isoform B). Both isoforms exhibited a cytoplasmic localization, although isoform B was also found concentrated in rod/donut-like structures devoid of actin or microtubules (Supporting Fig. S4C). Collectively, these results demonstrate that the participation of IMPDH in the catalytic biosynthesis of purines is necessary for HCC growth.

INTERTUMORAL HETEROGENEITY IN PURINE SYNTHETIC PATHWAY ACTIVITY DETERMINES TUMOR RESPONSE TO MPA

HCCs exhibit extensive heterogeneity with regards to proteomic, metabolomics, and immune profiles as well as responses to anticancer drugs, contributing to different metabolic requirements across tumors.^(31,32) We hypothesized that every tumor would thus have a unique growth dependency on IMPDH-driven purine biosynthesis and demonstrate varying sensitivities and tolerance toward MPA. PDX mouse models offer a clinically relevant system to test this hypothesis, with drug studies being able to be performed *in vivo* as well as *in vitro* on PDX organoids in the context of heterogeneous molecular alterations in patients. HCC cells from 13 patients were implanted into immunodeficient mice, and the characteristics of these distinct PDX lines were interrogated with respect to the status of purine metabolic activity (Fig. 3A). Immunoblotting performed on tumors validated the heterogeneous expression of

purine biosynthetic enzymes (Fig. 3B,C). Analysis of transcript levels yielded a tight correlation between messenger RNA (mRNA) and protein expression (Fig. 3D). We next measured the levels of metabolites in the purine metabolic pathway as a functional

readout of pathway activity. In agreement with protein and mRNA expression, the levels of metabolites in both the AMP and GMP branches showed comprehensive variation among PDX tumors, suggesting differential purine requirements for sustenance of tumor

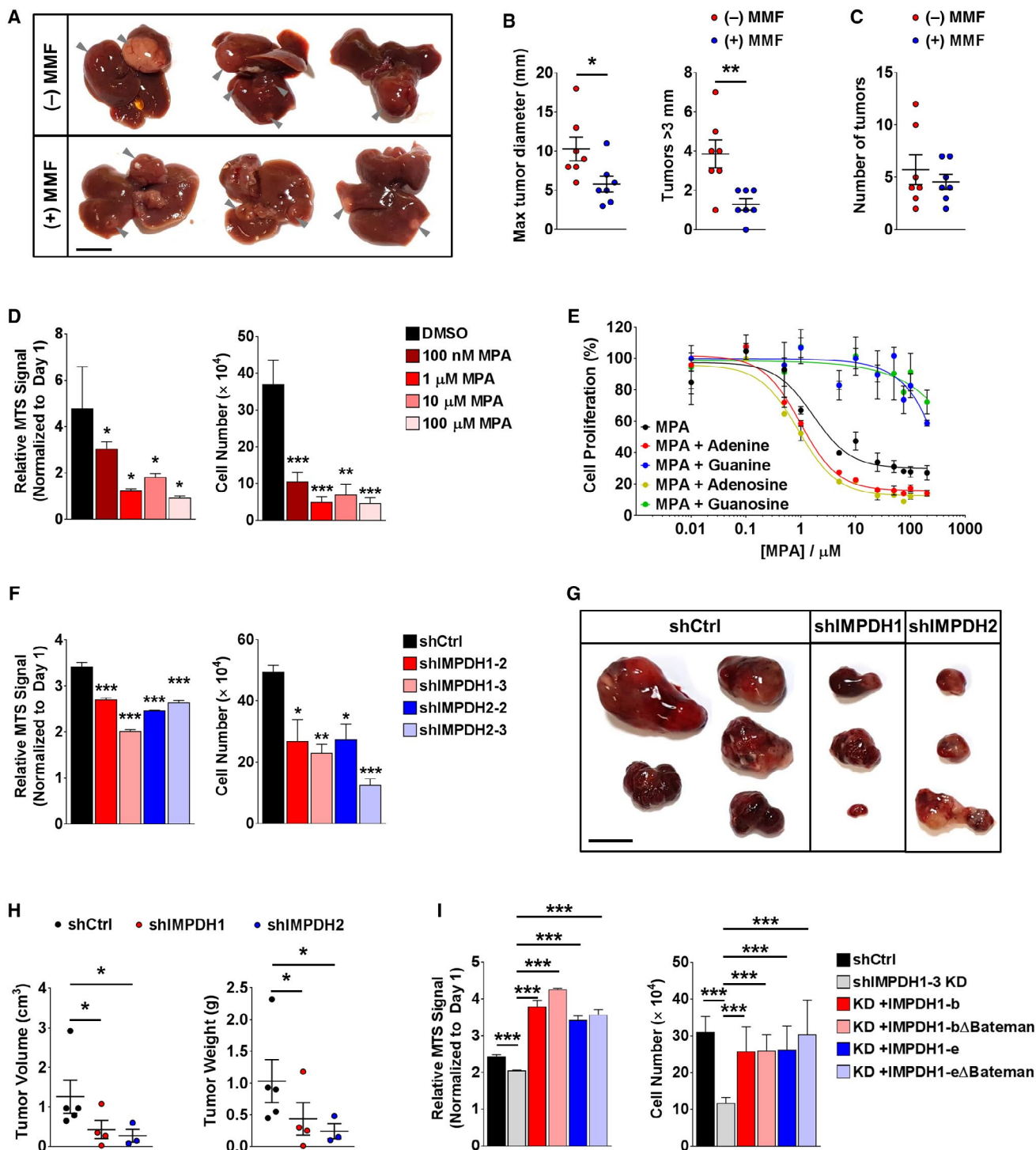


FIG. 2. Inhibition of IMPDH1/2 disrupts HCC proliferation and tumor progression. (A–C) Tumor burden in DEN-administered mice treated with vehicle control (–MMF) or MMF at a dosage of 120 mg/kg twice daily for 3 weeks (+MMF). (A) Macroscopic images of livers. Arrowhead indicates visible tumor nodule. Scale bar, 1 cm. (B,C) Quantification of (B) tumor size and (C) tumor multiplicity. (–) MMF, $n = 7$; (+) MMF, $n = 7$. (D) Dose-dependent cell-proliferative index of Huh7 cells 72 hours after exposure to MPA, quantified by MTS absorbance measurements and manual hemocytometer counting. (E) Dose-response curves of Huh7 cells to increasing concentrations of MPA with and without addition of adenine, guanine, adenosine, or guanosine (50 μ M). (F) Cell-proliferative index of Huh7 cells stably infected with a scrambled control or with two independent shRNA targeting *IMPDH1* (shIMPDH1) or *IMPDH2* (shIMPDH2), quantified by MTS absorbance measurements and manual hemocytometer counting. (G,H) Tumor burden in Huh7-derived xenografts in nude mice 1 month after subcutaneous injection with Huh7 shCtrl, shIMPDH1-3, or shIMPDH2-3 cells. (G) Macroscopic images of tumors. Scale bar, 1 cm. (H) Quantification of tumor volume and weight. shCtrl, $n = 5$; shIMPDH1, $n = 4$; shIMPDH2, $n = 3$. (I) Cell-proliferative index of Huh7 shIMPDH1-3 cells overexpressing two full-length IMPDH1 isoforms (IMPDH1-b/IMPDH1-e) or truncated IMPDH1 lacking the Bateman domain (IMPDH1-b Δ Bateman/IMPDH1-e Δ Bateman). Data are mean \pm SD; * $P < 0.05$, ** $P < 0.01$, *** $P < 0.001$. Abbreviation: KD, knockdown.

proliferation (Fig. 3E). A pairwise correlation analysis revealed that the purine metabolic signature correlated positively with genes involved in cellular proliferation (Fig. 3F), consistent with an oncogenic role for purine metabolism. Treatment with MPA of PDX tumors cultured as organoids dramatically inhibited the proliferation of some tumors (PDX #1 and #11) while exhibiting a negligible effect on others (PDX #12 and #19) (Fig. 3G). MPA treatment also resulted in elevation of the upstream metabolite 5-aminoimidazole-4-carboxamide-1- β -D-ribofuranoside (AICAR) in MPA-sensitive tumors (Fig. 3H), suggesting that AICAR levels could be a useful biomarker to monitor the effectiveness of MPA therapy. Intriguingly, PDX tumors that were MPA sensitive were characterized by two distinct features that implied tumor-specific vulnerabilities to IMPDH inhibition: elevated expression of either IMPDH1 or IMPDH2, and high levels of guanosine nucleosides.

PI3K SIGNALING REGULATES PURINE SYNTHETIC ENZYME EXPRESSION

Metabolic reprogramming of tumor cells is regulated by oncogenic pathways, activation of which enables tumor adaptation in an altered nutritional microenvironment to sustain rapid proliferation and evade apoptosis.⁽³³⁾ In this context, we tested a panel of drugs targeting oncogenic pathways previously implicated in cancer metabolic reprogramming on Huh7 shIMPDH1 and shIMPDH2 cells to identify signaling pathways that drive purine metabolism. The rationale for this was that down-regulated expression of IMPDH1 or IMPDH2 would lead to decreased purine synthetic activity, rendering increased

susceptibilities to a drug that inhibits a protein directly regulating the expression levels of purine synthetic enzymes. Given that purine metabolic activity is necessary for proliferation of Huh7 cells, a drug-induced reduction in enzyme levels would result in enhanced sensitivities of shIMPDH1 and shIMPDH2 cells in the same manner that these cells exhibited increased vulnerability to MPA, which has a higher affinity for IMPDH2 than IMPDH1 (3-fold and 13-fold decrease in median inhibitory concentration [IC_{50}] in shIMPDH1 and shIMPDH2 cells, respectively) (Fig. 4A). Indeed, only the PI3K inhibitor PI-103 conferred added vulnerability of Huh7 shIMPDH1 and shIMPDH2 cells (1.5-fold and 1.8-fold decrease in IC_{50} , respectively) (Fig. 4B). In contrast, IMPDH down-regulation did not alter Huh7 sensitivity to drugs targeting proteins previously shown to regulate HCC tumorigenesis (Supporting Fig. S5A–H). Importantly, Huh7 shIMPDH1 and shIMPDH2 cells were also resistant to mammalian target of rapamycin (mTOR) inhibition by rapamycin (Supporting Fig. S5I), suggesting that a PI3K-induced mTOR-independent signaling mechanism regulates purine synthesis in Huh7 cells.

We next examined the effect of PI-103 and protein kinase B (AKT) inhibitor MK-2206 on the expression of purine synthetic enzymes. Protein levels of ATIC, phosphoribosyl pyrophosphate synthetase 1 (PRPS1; functioning in the main branch leading to IMP generation), IMPDH1, IMPDH2 (involved in converting IMP to GMP), and ADSL (involved in converting IMP to AMP) were decreased in a dose-dependent fashion in Huh7 cells (Fig. 4C). This decrease was also observed at the mRNA level for all 11 purine synthetic enzymes (Supporting Fig. S6A). We observed a similar dependency in PDX #11 organoids (Fig. 4C), a

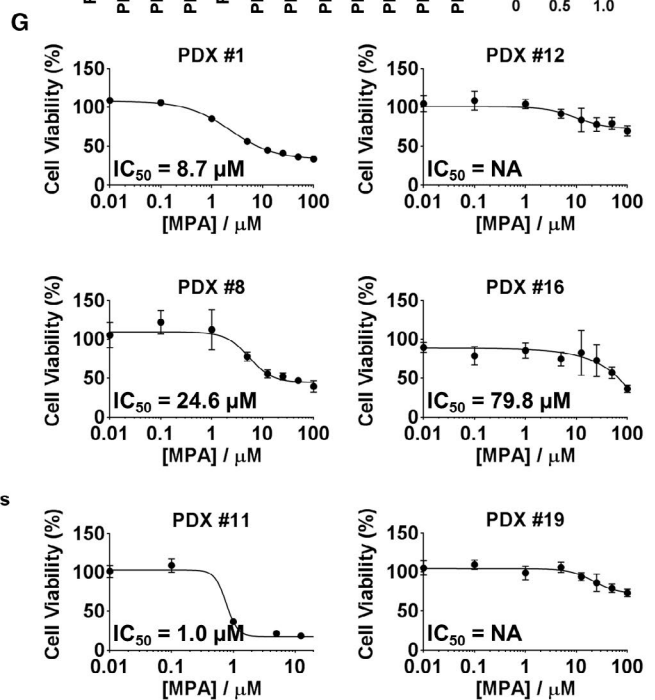
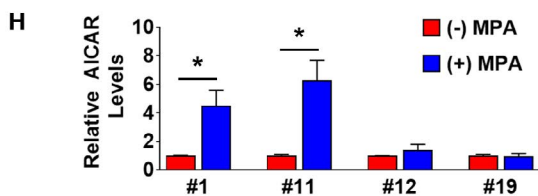
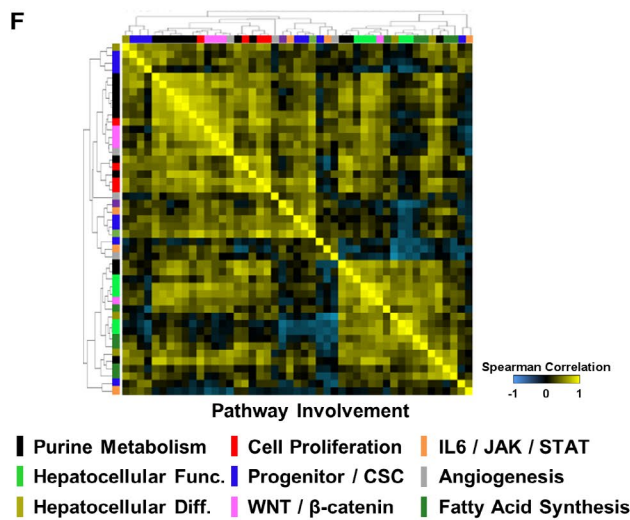
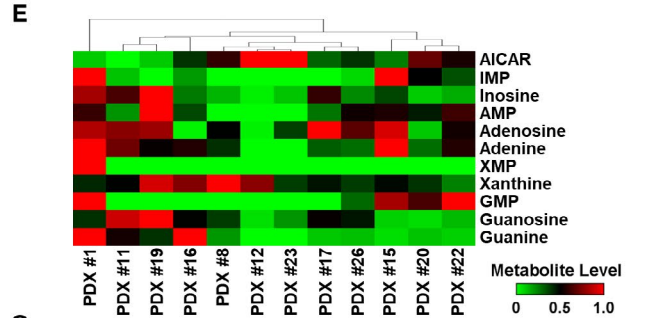
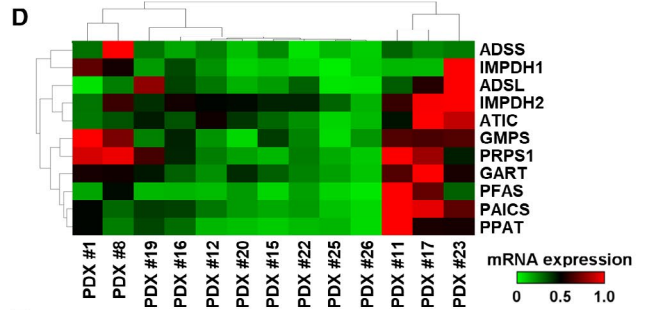
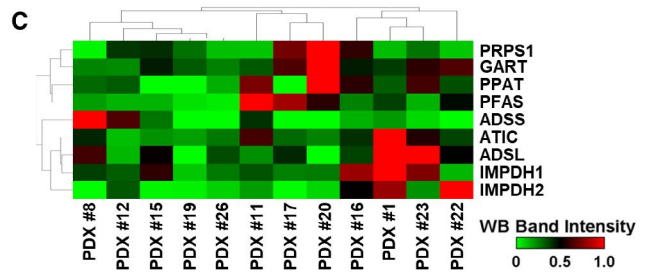
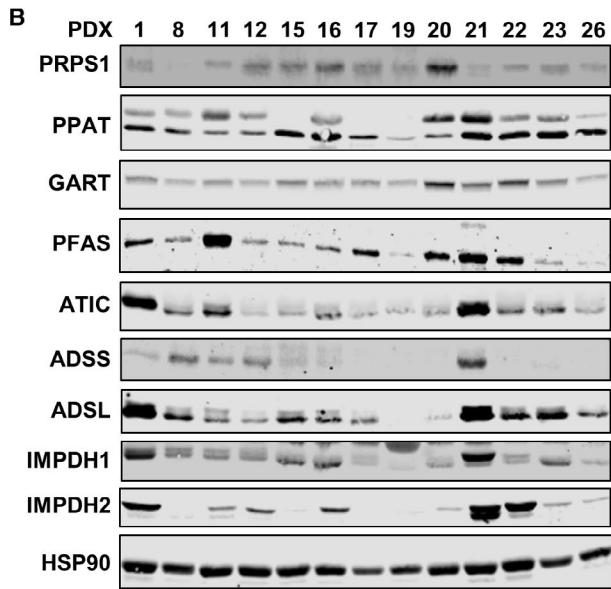
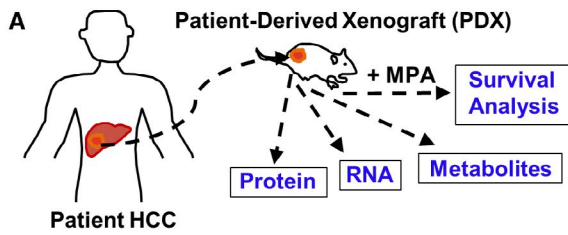


FIG. 3. Heterogeneous purine metabolism in HCC-PDX tumors determines tumor response to MPA. (A) Schema of the PDX workflow. (B) Western blot showing purine biosynthetic enzyme levels in PDX tumors. HSP90 is used as a loading control. (C-E) Heatmaps showing (C) western blot quantification, (D) transcript levels of purine biosynthesis pathway genes, and (E) levels of purine metabolites in PDX tumors. (F) Heatmap of clustered correlation matrix displaying Spearman rank correlations for the expression (qPCR) of HCC-essential genes in PDX tumors. The relationship distance between genes is ordered by hierarchical clustering. Genes involved in purine metabolism (black) were found to be highly correlated with cell proliferation (red). (G) Dose-response curves to MPA of PDX tumors cultured as organoids. Highly MPA-sensitive, $IC_{50} < 10 \mu M$; MPA-resistant, $IC_{50} = NA$. (H) Relative abundance of AICAR metabolites in PDX tumor organoids treated with $10 \mu M$ MPA for 24 hours. Data are mean \pm SD; * $P < 0.05$. Abbreviations: CSC, cancer stem cell; Diff, differential; Func, function; IL6, interleukin 6; JAK, Janus kinase; NA, not applicable; STAT, signal transducer and activator of transcription; WB, western blot.

patient-derived line most vulnerable to IMPDH inhibition (Fig. 3G). To mimic nutrient deprivation and insulin resistance in the tumor environment, we grew serum-starved Huh7 cells with 1 g/L glucose, which is one fifth the glucose concentration in standard cell culture conditions, in the presence of insulin. Under these conditions, elevated expression of purine synthetic enzymes was decreased to near baseline levels in cells treated with PI-103 (Fig. 4D). Importantly, overexpression of phosphatase and tensin homolog (PTEN), a negative regulator of PI3K signaling, in Huh7 cells also resulted in attenuated expression of purine synthetic enzymes (Supporting Fig. S6B). The tight association between PI3K signaling and purine synthesis prompted us to interrogate their relationship in the TCGA-LIHC cohort. Mutations in genes encoding PI3K pathway components, which alter the activation status or expression levels of the enzymes, are a frequent occurrence in cancers.⁽³⁴⁾ A pairwise correlation analysis revealed a strong correlation between the purine metabolic signature and PI3K pathway components (Fig. 4E). In addition, deleterious mutations in PI3K pathway components were enriched in tumors overexpressing purine synthetic enzymes (Supporting Fig. S6C), linking aberrant PI3K pathway activation to elevated expression of these enzymes. Decreased expression of the tumor suppressor *PTEN* and up-regulation of the oncogenic phosphoinositide-3-kinase regulatory subunit 6 (*PIK3R6*) also correlate with poor prognosis in HCC (Supporting Fig. S6D). Transcriptomic analysis of the SGH-HCC cohort revealed a similar correlation between purine biosynthetic and PI3K pathway genes (Supporting Fig. S6E). We next performed drug combination studies to determine if inhibitors of these pathways synergize in inhibiting Huh7 viability. Using the Chou-Talalay method,⁽³⁵⁾ the combination index values for the combination of PI-103 and MPA were 0.21 and 0.76 in Huh7 cells (Fig. 4F) and PDX #11 organoids (Fig. 4G), respectively, indicating

strong synergy. Taken together, these results establish the nonredundant requirement of purine synthesis on PI3K signaling in maintaining HCC proliferation and tumorigenesis.

E2F TRANSCRIPTION FACTOR 1 IS A DOWNSTREAM EFFECTOR OF PI3K SIGNALING IN THE REGULATION OF PURINE SYNTHESIS

The dispensability of mTOR for purine synthesis-dependent survival of Huh7 cells implied an mTOR-independent branch of PI3K signaling functioning to manipulate the expression of purine synthetic enzymes. To identify the PI3K effector activating gene transcription, we analyzed the gene promoters of all purine synthetic enzymes to identify top candidate transcription factor (TF) occupancy. We focused our analysis to only include sites that had published evidence of TF binding so as to select for TFs that demonstrate highest functional binding potential. mRNA down-regulation of all purine synthetic enzymes in response to PI3K inhibition (Supporting Fig. S6A) suggested a common TF, prompting us to compare across all 11 gene promoters, yielding cyclic adenosine monophosphate response element-binding protein (CREB), E2F transcription factor 1 (E2F1), and MYC as candidate TFs (Fig. 5A). MYC inhibition had no effect on the mRNA levels of genes encoding purine synthetic enzymes (Supporting Fig. S7A), whereas CREB inhibitor 666-15 resulted in a modest increase in transcript levels (Supporting Fig. S7B), suggesting that MYC and CREB binding to these loci occurred in a manner distinct and independent of PI3K regulation of purine synthesis pathway gene expression. In contrast, expression levels of these genes were down-regulated in a dose-dependent fashion in response to E2F1 inhibition by HLM006474 (Fig. 5B). *E2F1* knockdown using two independent

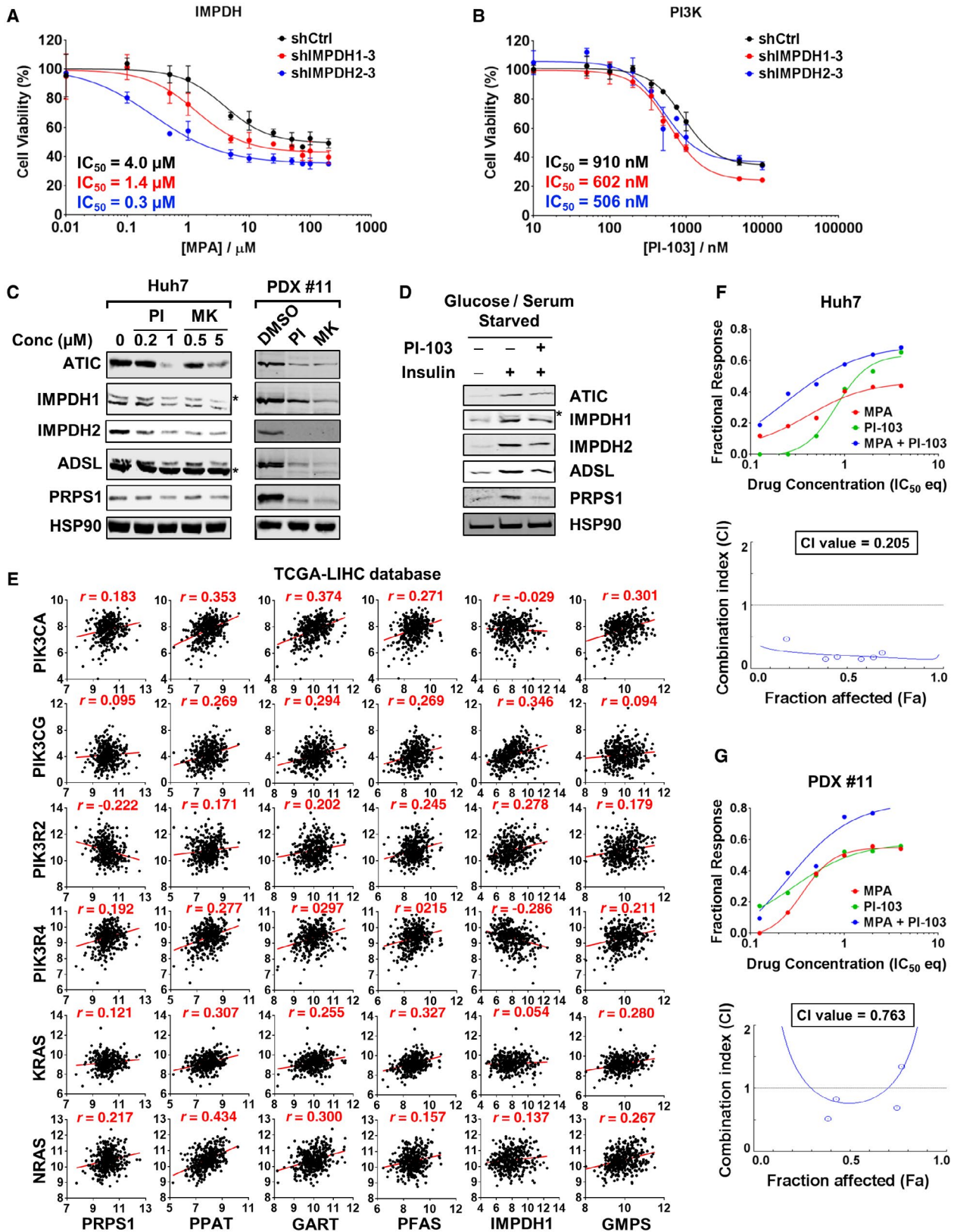


FIG. 4. PI3K signaling regulates purine biosynthesis pathway enzymes in HCC. (A,B) Dose-response curves to (A) MPA and (B) PI-103 of Huh7 control (black), shIMPDH1 (red), and shIMPDH2 (blue) cells. (C) Western blot showing decreased ATIC, IMPDH1, IMPDH2, ADSL, and PRPS1 levels in Huh7 cells (left panel) and PDX #11 organoids (right panel) treated with PI-103 and MK-2206 for 48 hours. For PDX #11 cells, 1 μ M PI-103 and 5 μ M MK-2206 were used. The * indicates a nonspecific band. (D) Western blot showing ATIC, IMPDH1, IMPDH2, ADSL, and PRPS1 levels in Huh7 cells under glucose and serum-restricted conditions (1 g/L glucose and 0.5% serum) and after addition of 100 nM insulin with or without 1 μ M PI-103 for 48 hours. (E) Pairwise correlation analysis of six representative genes in the PI3K signaling pathway (*PIK3CA*, *PIK3CG*, *PIK3R2*, *PIK3R4*, *KRAS*, and *NRAS*) and the purine synthesis pathway (*PRPS1*, *PPAT*, *GART*, *PFAS*, *IMPDH1*, and *GMPS*). Plots indicate gene expression data of patients from TCGA-LIHC. Spearman correlation coefficient (r) values are shown. (F,G) Combination index analysis with MPA and PI-103 in (F) Huh7 cells and (G) PDX #11 organoids. Upper graph shows dose-response curves. Drug-dependent inhibition of cell viability is plotted on the vertical axis as the fraction of cells affected by the drug treatment (Fa), and the drug concentration is plotted on the horizontal axis as a fraction of the IC₅₀. Lower graph shows Fa-CI plot generated using the Chou-Talalay method to determine the extent of synergy. Data are mean \pm SD. Abbreviations: CI, combination index; Conc, concentration; eq, equivalent; Fa, fraction affected; KRAS, KRAS proto-oncogene, guanosine triphosphatase; MK, MK-2206; NRAS, NRAS proto-oncogene, guanosine triphosphatase; PI, PI-103.

shRNAs also resulted in decreased expression of purine biosynthetic enzymes (Supporting Fig. S7C). PI-103 and HLM006474 treatment led to a decrease of E2F1 occupancy on the promoters of these genes (Fig. 5C,D). Combinatorial targeting of E2F1 and IMPDH using HLM006474 and MPA yielded synergism in both Huh7 cells and PDX #11 organoids (Fig. 5E,F) with combination index values of 0.60 and 0.67, respectively. A combination of HLM006474 and PI-103 was also synergistic in inhibiting the proliferation of Huh7 and PDX #11 cells (Fig. 5G,H), with combination index values of 0.51 and 0.60, respectively. E2F1 activity is regulated by interaction with the RB transcriptional corepressor (RB), whereby hyperphosphorylated RB dissociates from E2F1, allowing for E2F1-dependent transcription of target genes.^(36,37) Importantly, PI-103 treatment attenuated RB phosphorylation at four distinct sites in Huh7 and PDX #11 cells (Fig. 5I), supporting a role for PI3K signaling as an upstream driver in hyperphosphorylating RB and subsequent E2F1-mediated activation of genes in the purine synthesis pathway.

DOWN-REGULATION OF IMPDH ACTIVITY LEADS TO PREFERENTIAL INHIBITION OF MITOGEN-ACTIVATED PROTEIN KINASE/RAS SIGNALING

To understand how purine biosynthesis promotes HCC tumorigenesis, we performed RNA-sequencing on Huh7 shIMPDH1 and shIMPDH2 cells. Principal component analysis comparing the transcriptomes indicated marked differences in gene expression profiles despite similar proliferative impairment (Fig. 6A). Pairwise comparison of short

hairpin control (shCtrl) cells versus shIMPDH1 (Supporting Fig. S8A) or shIMPDH2 (Supporting Fig. S8B) cells showed that depletion of either IMPDH isoform was sufficient to induce large-scale alterations in gene expression, despite both isoforms having similar substrate kinetics for the conversion of IMP to XMP. Because *IMPDH1* or *IMPDH2* knockdown impacted Huh7 proliferation, we reasoned that signaling pathways specifically affected by perturbations in purine synthesis that contribute to tumor proliferation should be down-regulated in both Huh7 shIMPDH1 and shIMPDH2 cells. Gene ontology analysis revealed that mitogen-activated protein kinase (MAPK)/RAS signaling was the most significantly down-regulated signaling pathway (Fig. 6B). Reassuringly, genes associated with cell-cycle progression and regulation of cell proliferation were also significantly down-regulated. mRNA transcripts of MAPK/RAS pathway components were reduced by more than 2-fold in response to *IMPDH1* or *IMPDH2* knockdown (Fig. 6C,D). We next interrogated the clinical relevance of the association of MAPK/RAS signal activation with IMPDH expression levels in the TCGA-LIHC and SGH-HCC cohorts by performing a pairwise correlation between *IMPDH1* and genes of MAPK/RAS pathway components. We found that tumors with high *IMPDH1* levels were marked by elevated expression of MAPK/RAS pathway genes in both the TCGA-LIHC (Fig. 6E) and SGH-HCC data sets (Supporting Fig. S8C). Treating Huh7 cells with MPA and measuring downstream readouts of MAPK pathway activation revealed that IMPDH inhibition significantly decreased phosphorylation of MAPK substrates on both threonine and

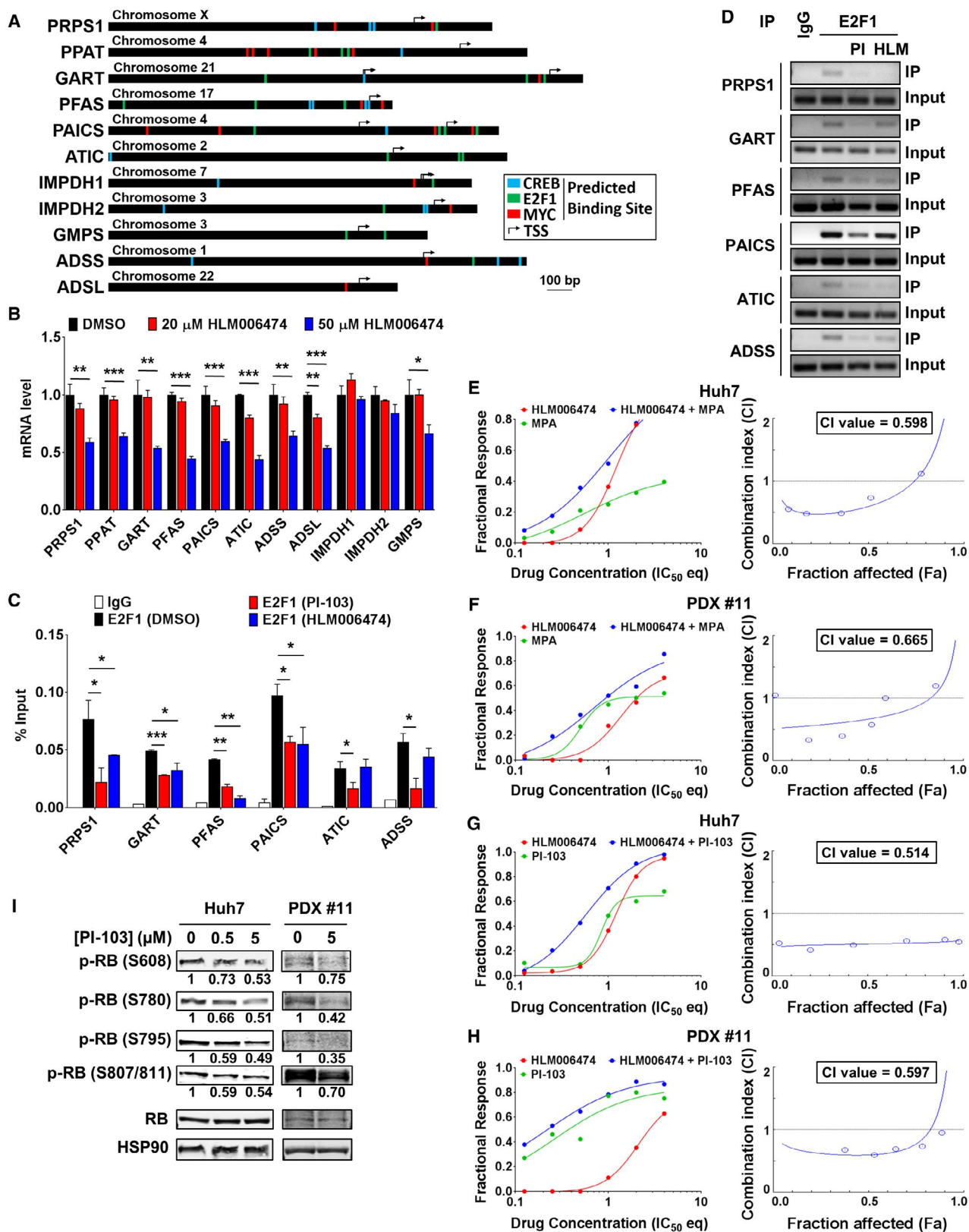


FIG. 5. E2F1 acts downstream of PI3K to regulate purine biosynthesis pathway enzymes in HCC. (A) The promoters of the 11 purine biosynthesis pathway genes showing the binding sites of CREB (blue), E2F1 (green), and MYC (red) in relation to the transcription start site. (B) Expression of purine biosynthesis pathway genes in Huh7 cells treated with DMSO or HLM006474 for 24 hours. (C,D) Chromatin immunoprecipitation of E2F1 and IgG control in Huh7 cells treated with DMSO, PI-103 (1 μ M), or HLM006474 (20 μ M) for 24 hours. Promoter expression levels of six representative genes in the purine synthesis pathway (*PRPS1*, *GART*, *PFAS*, *PAICS*, *ATIC*, and *ADSS*) in the immunoprecipitated chromatin normalized to input chromatin are determined by (C) qPCR and (D) semiquantitative PCR analyzed on a 2.5% agarose gel. (E,F) Combination index analysis with HLM006474 and MPA in (E) Huh7 cells and (F) PDX #11 organoids. Graph on the left shows dose-response curves. Graph on the right shows Fa-CI plot to determine the extent of synergy. (G,H) Combination index analysis with HLM006474 and PI-103 in (G) Huh7 cells and (H) PDX #11 organoids. (I) Western blot showing decreased phosphorylation of RB on four C-terminal phosphorylation sites (S608, S780, S795, and S807/S811) in Huh7 cells and PDX #11 organoids treated with PI-103 for 2 hours. p-RB band intensity is quantified and normalized to RB. Data are mean \pm SD; * P < 0.05, ** P < 0.01, *** P < 0.001. Abbreviations: AREG, amphiregulin; AXIN2, axin 2; BAX, BCL2 associated X, apoptosis regulator; bp, base pair; CACNB3, calcium voltage-gated channel auxiliary subunit beta 3; CACNG4, calcium voltage-gated channel auxiliary subunit gamma 4; CCND1, cyclin D1; CI, combination index; DDX18, DEAD-box helicase 18; DUSP4, dual specificity phosphatase 4; DUSP6, dual specificity phosphatase 6; EFNA3, ephrin A3; EGR1, early growth response 1; EPHA2, EPH receptor A2; eq, equivalent; Fa, fraction affected; FGFR2, fibroblast growth factor receptor 2; FLNA, filamin A; FOS, Fos proto-oncogene, AP-1 transcription factor subunit; GLUL, glutamate-ammonia ligase; GRB2, growth factor receptor bound protein 2; HLM, HLM006474; IgG, immunoglobulin G; IP, immunoprecipitation; JUNB, JunB proto-oncogene, AP-1 transcription factor subunit; LDHA, lactate dehydrogenase A; p, phosphorylated; PDGFA, platelet derived growth factor subunit A; PDGFB, platelet derived growth factor subunit B; PDGFRA, platelet derived growth factor receptor alpha; PI, PI-103; RASGRP2, RAS guanyl releasing protein 2; SPRY4, sprouty RTK signaling antagonist 4; TBX3, T-box transcription factor 3; TIMP2, TIMP metalloproteinase inhibitor 2; TSS, transcription start site.

serine residues in consensus MAPK phosphorylation motifs as well as phosphorylation of p44 MAPK (ERK1) (Fig. 6F). MPA also resulted in decreased MAPK target gene expression (Fig. 6G). The minimal effect on wingless-related integration site (WNT) and MYC target genes supports MAPK signaling as a selective signaling pathway dependent on active purine biosynthesis. Such gradation of pathway dependencies rules out a global deregulation of oncogenic pathways in response to antagonism of purine metabolism.

COMBINATORIAL TARGETING OF PURINE BIOSYNTHESIS INHIBITS *IN VIVO* HCC TUMORIGENESIS

Our data suggest a critical role for purine biosynthesis in the proliferation of HCC cells, mediated in part by a PI3K–E2F1 axis that precisely regulates purine biosynthetic enzyme expression. Given that PI3K inhibition only partially blocks the expression of these enzymes but combining PI-103 with MPA synergistically inhibited HCC cell viability, we hypothesized that efficient blockage of purine biosynthetic enzyme output through the cooperative action of MPA and PI-103 is critical for abrogating HCC tumor growth. To this end, we investigated the *in vivo* efficacy of combinatorial impediment of purine biosynthesis in a PDX mouse model. Mice transplanted with PDX #11 tumor cells were

subjected to one of four arms of treatment for 3 weeks: vehicle control, MMF monotherapy, PI-103 monotherapy, or a combination of MMF (120 mg/kg twice a day) and PI-103 (10 mg/kg daily) (Fig. 7A). Compared to vehicle control, the tumor burden was decreased in animals receiving either monotherapy regimen. Importantly, we observed strongest reduction in tumor growth in the cohort that received the drug combination (Fig. 7B,C). Histologic analysis revealed a loss of normal cord architecture in vehicle-treated tumors that was partially negated in the group administered the combinatorial therapy (Fig. 7D), demonstrating the efficacy of sustained and targeted inhibition of purine biosynthesis in HCC.

Discussion

Elevated energy consumption of tumor cells to support rapid proliferation necessitates the integration of various metabolic processes to sustain high levels of DNA replication and RNA production.⁽⁶⁾ In this study, we found that HCCs up-regulate enzymes involved in purine metabolism. Such coordinated increased expression of all enzymes in the pathway, as opposed to regulation of purine synthesis through modulation of a single enzyme, is significant in the context of cancer metabolism because alterations in metabolic flux are often achieved by the actions of an upstream master transcriptional regulator to effect a

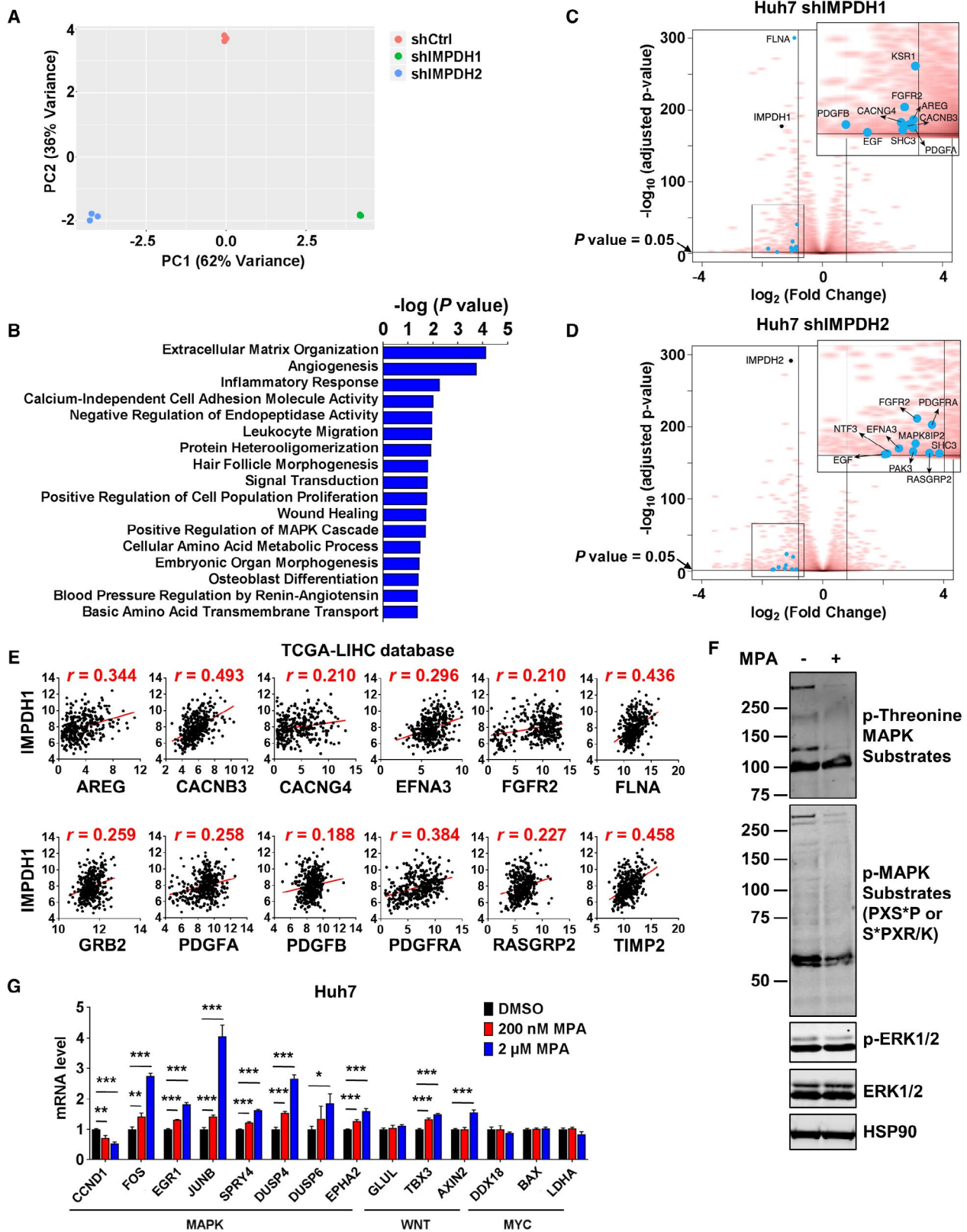


FIG. 6. Purine biosynthesis regulates MAPK/RAS signaling in HCC. (A) Principle component analysis comparing transcriptomes of Huh7 control, shIMPDPH1-3, or shIMPDPH2-3 cells. Each dot represents a biological replicate. (B) Significantly enriched biological processes (Gene Ontology) of down-regulated genes common to Huh7 shIMPDPH1 and shIMPDPH2 cells relative to shCtrl cells. (C,D) Volcano plot showing down-regulated expression of genes in the MAPK/RAS signaling pathway in (C) Huh7 shIMPDPH1 and (D) shIMPDPH2 cells. Boxed region has been magnified for clarity. (E) Pairwise correlation analysis of *IMPDPH1* and MAPK/RAS signaling pathway genes. Plots indicate gene expression data of patients from TCGA-LIHC. Spearman correlation coefficient (r) values are shown. (F) Western blot showing decreased phosphorylation of ERK1 (p44), and MAPK target substrates in Huh7 cells treated with 1 μ M MPA for 24 hours. PXS*P and S*PXR/K are consensus MAPK phosphorylation sites. (G) Expression of MAPK/RAS, WNT, and MYC target genes in Huh7 cells treated with MPA for 24 hours. Data are mean \pm SD; * $P < 0.05$, ** $P < 0.01$, *** $P < 0.001$. Abbreviations: p, phosphorylated; PC, principle component; WNT, wingless-related integration site.

synchronized and efficient mode of control over the entire synthetic pathway.⁽³⁸⁾ MYC has been shown to transcriptionally regulate purine biosynthesis in various cancers.⁽⁹⁻¹²⁾ However, MYC does not perform a similar role in HCC. Instead, we report a PI3K–E2F1 axis, suppression of which antagonized the activation of the entire suite of purine synthetic genes to repress HCC tumorigenesis. Identification of PI3K signaling as a master regulator of purine metabolism is significant because aberrant activation of this network occurs frequently in cancers to decouple deregulated tumor cell growth from the external nutritional milieu.⁽³⁹⁾ PI3K–mTOR signaling is an essential driver of cancer metabolic reprogramming, in part through integration of glycolytic intermediates into purine synthesis.⁽⁴⁰⁾ It was therefore surprising that mTOR inhibition did not significantly alter HCC viability in the setting of purine synthesis inhibition, consistent with a previous report showing a mode of PI3K regulation of purine synthesis independent of mTOR/S6 kinase in mouse embryonic fibroblasts and C2C12 myoblasts.⁽⁴¹⁾ In the context of HCC, a recent study comparing the responses of 81 HCC cell lines to a panel of anticancer drugs demonstrated that, despite rapamycin and PI-103 eliciting similar sensitivities in many lines, a significant fraction exhibited opposing vulnerabilities to PI3K or mTOR inhibition,⁽³¹⁾ attesting to a subset of HCC wherein mTOR is dispensable for PI3K regulation. Here, we demonstrate that PI3K signaling modulates E2F1 occupancy on purine synthetic gene promoters through RB phosphorylation, thus relieving sequestration of E2F1 to RB, consistent with a role for E2F1 in regulating the cell cycle and metabolic adaptations of cancer cells.⁽⁴²⁾ The effect of PI3K signaling on RB phosphorylation is likely mediated by the cyclin D–cyclin-dependent kinase 4/6 complex⁽⁴³⁾ because we find no evidence of AKT phosphorylation sites on RB. Elevated expression levels and copy number gains in E2F1 in high-grade HCCs^(44,45) are consistent with

our analysis of the TCGA-LIHC data set where we found up-regulation of purine synthetic enzymes in high-grade HCC, further highlighting a functional link between E2F1 and purine synthesis in promoting HCC malignancy. Taken together, we establish a central role for E2F1 at the interface of oncogenic signal transduction and tumor metabolism. In light of our findings that PI3K inhibition is sufficient to repress the purine synthetic gene expression stimulated by excess insulin, it is tempting to speculate a link between insulin resistance and HCC pathogenesis that is mediated by PI3K-regulated purine synthesis.

Preferential exploitation of purine synthesis to propagate HCC tumorigenesis suggests that purine metabolism offers a point of vulnerability to therapeutically target HCC. Conventional therapies have not yielded dramatic improvements in survival cohort studies.^(3,4) This is probably due to extensive tumor heterogeneity as well as a complex interplay among oncogenic signaling pathways and metabolic reprogramming. Indeed, our findings that attenuation of purine synthesis resulted in preferential down-regulation of MAPK/RAS signaling rather than a global deregulation of cell signaling hints at a convergence of the effects of purine metabolism on nucleic acid synthesis and the generation of secondary messenger cyclic (c)AMP and cGMP. In this context, treatment with cAMP target protein kinase A agonist forskolin affected MAPK pathway activity and subsequent mitogenesis in HCC cell lines,⁽⁴⁶⁾ and frequent activation and up-regulation of MAPK pathway components are detected in HCCs.^(47,48) Taken together, attenuated MAPK signal transduction in response to the inhibition of purine synthesis likely plays a significant role toward decreased HCC tumorigenesis, although the contributions of other signaling pathways should not be discounted.

Given the limited success of current therapies, it is noteworthy that we observe trifurcation of PDX tumor response toward MPA treatment, suggesting

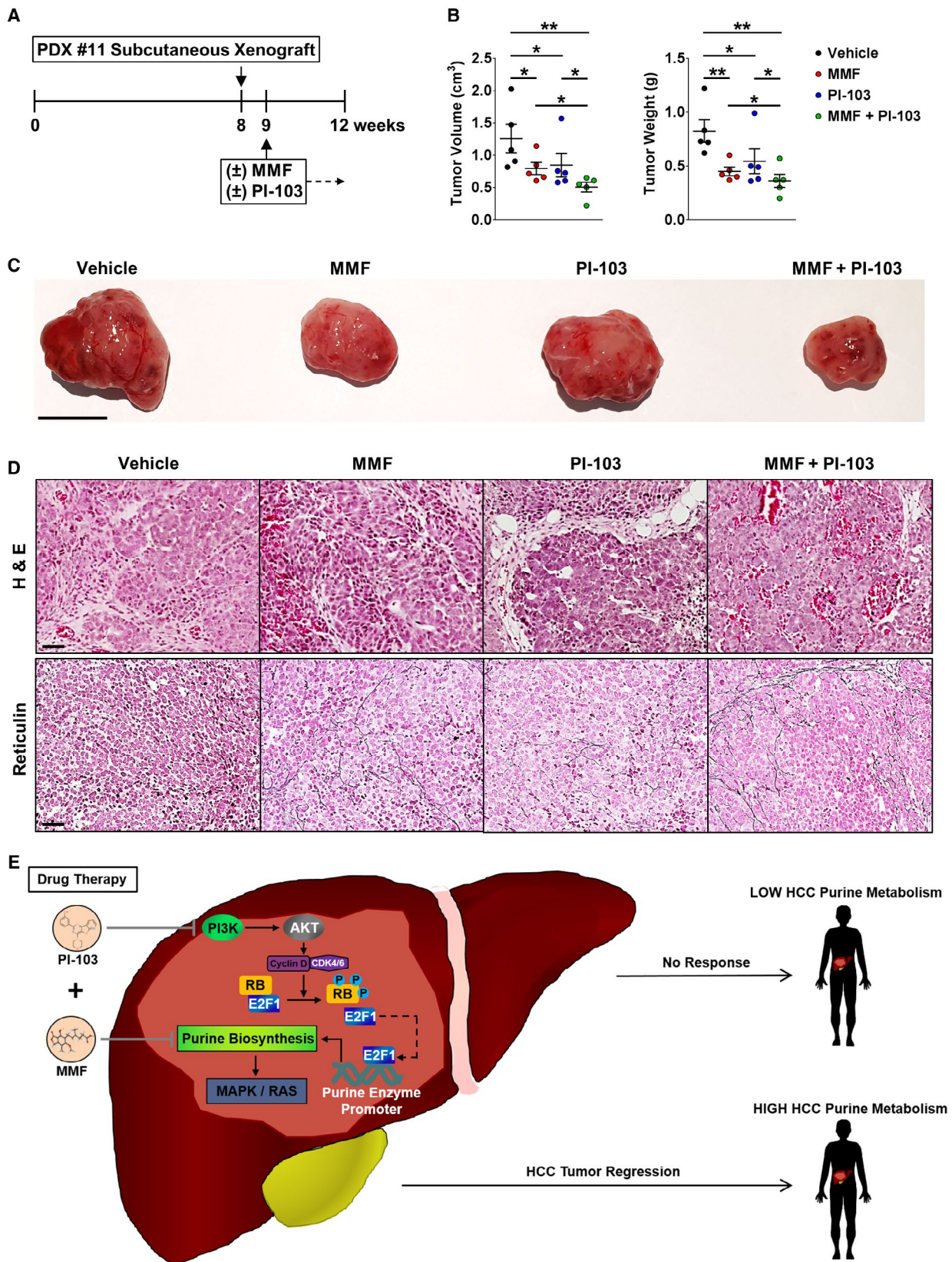


FIG. 7. Combined targeting of purine biosynthesis inhibits *in vivo* HCC tumorigenesis. (A) Workflow of MMF and PI-103 administration in NSG mice subcutaneously transplanted with PDX #11 tumor cells. (B,C) Tumor burden in NSG mice bearing PDX #11 xenografts treated with vehicle control, MMF monotherapy (120 mg/kg twice a day), PI-103 monotherapy (10 mg/kg daily), or a combination of MMF (120 mg/kg twice a day) and PI-103 (10 mg/kg daily). (B) Quantification of tumor volume and weight; n = 5 per treatment group. Data are mean \pm SD; * $P < 0.05$, ** $P < 0.01$. (C) Representative macroscopic images of tumors. Scale bar, 1 cm. (D) Representative images of H&E and reticulin-stained sections. Scale bar, 50 μ m. (E) Model depicting PI3K–E2F1 regulation of purine biosynthetic enzymes to drive HCC tumorigenesis. Combinatorial targeting using MMF and PI-103 is most effective in suppressing tumor growth in patients with HCC with enhanced purine metabolism. Abbreviation: H&E, hematoxylin and eosin.

that targeting of purine synthesis is most effective in a subset of patients. This distinction in tumor response can be accounted for by the graded expression of purine synthetic enzymes and metabolites in the PDX tumors, indicative of patient-specific requirements for purine synthesis in driving HCC tumorigenesis. A comparison of proteomic and metabolomic expression in MPA-resistant and susceptible PDX tumors suggests that tumors that respond to IMPDH inhibition are defined by two features: elevated expression of IMPDH1 or IMPDH2, and high guanosine levels. Conversely, tumors resistant to MPA express either low guanosine levels despite high IMPDH1 and IMPDH2 expression (PDX #12) or exhibit elevated guanosine levels despite no detectable IMPDH1 or IMPDH2 (PDX #19). This discrepancy might be accounted for by the enhanced contribution of the purine salvage pathway, allowing for the IMPDH-independent generation of guanosine nucleosides from byproducts of DNA and RNA degradation. Collectively, this suggests that enhanced levels of both IMPDH1/IMPDH2 and guanosine could serve as potential biomarkers to inform the design of personalized therapy for patients with HCC to select those most likely to benefit from MMF treatment. It is also noteworthy that we observed increased AICAR levels in MPA-sensitive tumors following MPA treatment, suggesting a potential utility of AICAR measurement as a proxy to measure the effectiveness of IMPDH inhibition.

An improvement over the use of a single therapeutic agent is the combinatorial approach of simultaneously targeting a key rate-limiting step in purine synthesis driven by IMPDH and an upstream oncogenic regulator to enhance the antitumorigenic efficacy. In this regard, a recent study demonstrated the benefit of blocking pyrimidine synthesis using teriflunomide in conjunction with PI3K inhibitor BKM120 to increase the inhibition of glioblastoma tumorigenesis in a xenograft model.⁽⁴⁹⁾ For our study, we observed

a synergistic effect of combining MPA with PI-103 or HLM006474 in attenuating the proliferation of Huh7 cells and a PDX organoid culture (PDX #11). PDX #11 exhibited highest inherent purine synthetic activity among all PDX lines and therefore had the most severely impacted viability by MPA treatment. We subsequently showed that the tumor burden in a PDX #11 mouse model was reduced to a greater extent by cooperatively targeting purine biosynthesis using MMF and PI-103 compared to either monotherapy. Our results, as summarized in Fig. 7E, demonstrate a preferential requirement for purine synthesis mediated by the activities of PI3K and E2F1 in the proliferation and survival of a subset of patients with HCC. This offers a tantalizing approach to delivering precision therapy to patients by targeted inhibition of purine metabolism at two distinct points of susceptibility.

Acknowledgment: We thank A. Tan, W.K. Tham, and S. Adav for technical and experimental support. We also acknowledge the Singapore Bioimaging Consortium–Nikon Imaging Center for help with microscopy and image analysis.

REFERENCES

- 1) Bray F, Ferlay J, Soerjomataram I, Siegel RL, Torre LA, Jemal A. Global cancer statistics 2018: GLOBOCAN estimates of incidence and mortality worldwide for 36 cancers in 185 countries. *CA Cancer J Clin* 2018;68:394–424.
- 2) Belghiti J, Kianmanesh R. Surgical treatment of hepatocellular carcinoma. *HPB (Oxford)* 2005;7:42–49.
- 3) Llovet JM, Ricci S, Mazzaferro V, Hilgard P, Gane E, Blanc JF, et al.; SHARP Investigators Study Group. Sorafenib in advanced hepatocellular carcinoma. *N Engl J Med* 2008;359:378–390.
- 4) Kudo M, Finn RS, Qin S, Han KH, Ikeda K, Piscaglia F, et al. Lenvatinib versus sorafenib in first-line treatment of patients with unresectable hepatocellular carcinoma: a randomised phase 3 non-inferiority trial. *Lancet* 2018;391:1163–1173.
- 5) Llovet JM, Hernandez-Gea V. Hepatocellular carcinoma: reasons for phase III failure and novel perspectives on trial design. *Clin Cancer Res* 2014;20:2072–2079.
- 6) DeBerardinis RJ, Chandel NS. Fundamentals of cancer metabolism. *Sci Adv* 2016;2:e1600200.

- 7) Koppenol WH, Bounds PL, Dang CV. Otto Warburg's contributions to current concepts of cancer metabolism. *Nat Rev Cancer* 2011;11:325-337.
- 8) **Luengo A, Gui DY**, Vander Heiden MG. Targeting metabolism for cancer therapy. *Cell Chem Biol* 2017;24:1161-1180.
- 9) **Wang X, Yang K**, Xie Q, Wu Q, Mack SC, Shi Y, et al. Purine synthesis promotes maintenance of brain tumor initiating cells in glioma. *Nat Neurosci* 2017;20:661-673.
- 10) **Mannava S, Grachtchouk V**, Wheeler LJ, Im M, Zhuang D, Slavina EG, et al. Direct role of nucleotide metabolism in C-MYC-dependent proliferation of melanoma cells. *Cell Cycle* 2008;7:2392-2400.
- 11) Liu YC, Li F, Handler J, Huang CR, Xiang Y, Neretti N, et al. Global regulation of nucleotide biosynthetic genes by c-Myc. *PLoS One* 2008;3:e2722.
- 12) Barfeld SJ, Fazli L, Persson M, Marjavaara L, Urbanucci A, Kaukonen KM, et al. Myc-dependent purine biosynthesis affects nucleolar stress and therapy response in prostate cancer. *Oncotarget* 2015;6:12587-12602.
- 13) Weber G. Enzymes of purine metabolism in cancer. *Clin Biochem* 1983;16:57-63.
- 14) Zimmermann AG, Gu JJ, Laliberte J, Mitchell BS. Inosine-5'-monophosphate dehydrogenase: regulation of expression and role in cellular proliferation and T lymphocyte activation. *Prog Nucleic Acid Res Mol Biol* 1998;61:181-209.
- 15) Jayaram HN, Dion RL, Glazer RI, Johns DG, Robins RK, Srivastava PC, et al. Initial studies on the mechanism of action of a new oncolytic thiazole nucleoside, 2-beta-D-ribofuranosylthiazole-4-carboxamide (NSC 286193). *Biochem Pharmacol* 1982;31:2371-2380.
- 16) Ahluwalia GS, Jayaram HN, Plowman JP, Cooney DA, Johns DG. Studies on the mechanism of action of 2-beta-D-ribofuranosylthiazole-4-carboxamide-V. Factors governing the response of murine tumors to tiazofurin. *Biochem Pharmacol* 1984;33:1195-1203.
- 17) Brazelton TR, Morris RE. Molecular mechanisms of action of new xenobiotic immunosuppressive drugs: tacrolimus (FK506), sirolimus (rapamycin), mycophenolate mofetil and leflunomide. *Curr Opin Immunol* 1996;8:710-720.
- 18) D'Cruz DP, Khamashta MA, Hughes GR. Systemic lupus erythematosus. *Lancet* 2007;369:587-596.
- 19) Cancer Genome Atlas Research Network. Comprehensive and integrative genomic characterization of hepatocellular carcinoma. *Cell* 2017;169:1327-1341.e1323.
- 20) Yates LR, Seoane J, Le Tourneau C, Siu LL, Marais R, Michiels S, et al. The European Society for Medical Oncology (ESMO) precision medicine glossary. *Ann Oncol* 2018;29:30-35.
- 21) European Association for the Study of the Liver, European Organisation for Research and Treatment of Cancer. EASL-EORTC clinical practice guidelines: management of hepatocellular carcinoma. *J Hepatol* 2012;56:908-943.
- 22) **Fong ELS, Toh TB**, Lin QXX, Liu Z, Hooi L, Mohd Abdul Rashid MB, et al. Generation of matched patient-derived xenograft in vitro-in vivo models using 3D macroporous hydrogels for the study of liver cancer. *Biomaterials* 2018;159:229-240.
- 23) Hu J, Locasale JW, Bielas JH, O'Sullivan J, Sheahan K, Cantley LC, et al. Heterogeneity of tumor-induced gene expression changes in the human metabolic network. *Nat Biotechnol* 2013;31:522-529.
- 24) Chong YC, Lim TE, Fu Y, Shin EM, Tergaonkar V, Han W. Indian Hedgehog links obesity to development of hepatocellular carcinoma. *Oncogene* 2019;38:2206-2222.
- 25) **Rhodes DR, Yu J**, Shanker K, Deshpande N, Varambally R, Ghosh D, et al. ONCOMINE: a cancer microarray database and integrated data-mining platform. *Neoplasia* 2004;6:1-6.
- 26) Roessler S, Jia HL, Budhu A, Forgues M, Ye QH, Lee JS, et al. A unique metastasis gene signature enables prediction of tumor relapse in early-stage hepatocellular carcinoma patients. *Cancer Res* 2010;70:10202-10212.
- 27) **Ghandi M, Huang FW**, Jane-Valbuena J, Kryukov GV, Lo CC, McDonald ER 3rd, et al. Next-generation characterization of the cancer cell line encyclopedia. *Nature* 2019;569:503-508.
- 28) Glesne DA, Collart FR, Huberman E. Regulation of IMP dehydrogenase gene expression by its end products, guanine nucleotides. *Mol Cell Biol* 1991;11:5417-5425.
- 29) Kozhevnikova EN, van der Knaap JA, Pindyurin AV, Ozgur Z, van Ijcken WF, Moshkin YM, et al. Metabolic enzyme IMPDH is also a transcription factor regulated by cellular state. *Mol Cell* 2012;47:133-139.
- 30) Thomas EC, Gunter JH, Webster JA, Schieber NL, Oorschot V, Parton RG, et al. Different characteristics and nucleotide binding properties of inosine monophosphate dehydrogenase (IMPDH) isoforms. *PLoS One* 2012;7:e51096.
- 31) **Qiu Z, Li H, Zhang Z**, Zhu Z, He S, Wang X, et al. A Pharmacogenomic landscape in human liver cancers. *Cancer Cell* 2019;36:179-193.e111.
- 32) **Zhang Q, Lou Y, Yang J**, Wang J, Feng J, Zhao Y, et al. Integrated multiomic analysis reveals comprehensive tumour heterogeneity and novel immunophenotypic classification in hepatocellular carcinomas. *Gut* 2019;68:2019-2031.
- 33) Tarrado-Castellarnau M, de Atauri P, Cascante M. Oncogenic regulation of tumor metabolic reprogramming. *Oncotarget* 2016;7:62726-62753.
- 34) Yuan TL, Cantley LC. PI3K pathway alterations in cancer: variations on a theme. *Oncogene* 2008;27:5497-5510.
- 35) Chou TC, Talalay P. Quantitative analysis of dose-effect relationships: the combined effects of multiple drugs or enzyme inhibitors. *Adv Enzyme Regul* 1984;22:27-55.
- 36) Chellappan SP, Hiebert S, Mudryj M, Horowitz JM, Nevins JR. The E2F transcription factor is a cellular target for the RB protein. *Cell* 1991;65:1053-1061.
- 37) Dyson N. The regulation of E2F by pRB-family proteins. *Genes Dev* 1998;12:2245-2262.
- 38) Lane AN, Fan TW. Regulation of mammalian nucleotide metabolism and biosynthesis. *Nucleic Acids Res* 2015;43:2466-2485.
- 39) Hoxhaj G, Manning BD. The PI3K-AKT network at the interface of oncogenic signalling and cancer metabolism. *Nat Rev Cancer* 2020;20:74-88.
- 40) Ben-Sahra I, Manning BD. mTORC1 signaling and the metabolic control of cell growth. *Curr Opin Cell Biol* 2017;45:72-82.
- 41) Wang W, Fridman A, Blackledge W, Connelly S, Wilson IA, Pilz RB, et al. The phosphatidylinositol 3-kinase/akt cassette regulates purine nucleotide synthesis. *J Biol Chem* 2009;284:3521-3528.
- 42) Denechaud PD, Fajas L, Giral A. E2F1, a novel regulator of metabolism. *Front Endocrinol (Lausanne)* 2017;8:311.
- 43) Averous J, Fonseca BD, Proud CG. Regulation of cyclin D1 expression by mTORC1 signaling requires eukaryotic initiation factor 4E-binding protein 1. *Oncogene* 2008;27:1106-1113.
- 44) **Kent LN, Bae S, Tsai SY**, Tang X, Srivastava A, Koivisto C, et al. Dosage-dependent copy number gains in E2f1 and E2f3 drive hepatocellular carcinoma. *J Clin Invest* 2017;127:830-842.
- 45) **Huang YL, Ning G, Chen LB**, Lian YF, Gu YR, Wang JL, et al. Promising diagnostic and prognostic value of E2Fs in human hepatocellular carcinoma. *Cancer Manag Res* 2019;11:1725-1740.
- 46) Schmidt CM, McKillop IH, Cahill PA, Sitzmann JV. The role of cAMP-MAPK signalling in the regulation of human hepatocellular carcinoma growth in vitro. *Eur J Gastroenterol Hepatol* 1999;11:1393-1399.
- 47) Ito Y, Sasaki Y, Horimoto M, Wada S, Tanaka Y, Kasahara A, et al. Activation of mitogen-activated protein kinases/extracellular

signal-regulated kinases in human hepatocellular carcinoma. *Hepatology* 1998;27:951-958.

- 48) Calvisi DF, Ladu S, Gorden A, Farina M, Conner EA, Lee JS, et al. Ubiquitous activation of Ras and Jak/Stat pathways in human HCC. *Gastroenterology* 2006;130:1117-1128.
- 49) **Wang X, Yang K**, Wu Q, Kim LJY, Morton AR, Gimple RC, et al. Targeting pyrimidine synthesis accentuates molecular therapy response in glioblastoma stem cells. *Sci Transl Med* 2019;11:eaau4972.

Author names in bold designate shared co-first authorship.

Supporting Information

Additional Supporting Information may be found at onlinelibrary.wiley.com/doi/10.1002/hep4.1559/supinfo.